PHYSICAL REVIEW B VOLUME 53, NUMBER 19 15 MAY 1996-I

Quasi-two-dimensional electron gas: Exchange and correlation energies

O. Betbeder-Matibet and M. Combescot
Groupe de Physique des Solides, Université Denis Diderot and Université Pierre et Marie Curie, CNRS, Tour 23, 2, place Jussieu, 75251 Paris Cedex 05, France

C. Tanguy
France Telecom, Centre National d'Etudes des Télécommunications, Paris B, Laboratoire de Bagneux, Boîte Postale 107, 92225 Bagneux Cedex, France

(Received 27 November 1995)

We calculate the $T=0$ exchange energy and correlation energy leading term of a quasi-two-dimensional electron gas localized in a doped semiconductor quantum well, taking into account the finite well width. Here we consider electron densities low enough to have electrons in one subband only. [S0163-1829(96)06119-X]

The exchange and correlation energies of an exact two-dimensional (2D) electron gas at $T=0$ were calculated long ago[1–4] as an expansion in the 2D average distance r_s defined as

$$n_s\pi(r_s a_0)^2=1, \tag{1}$$

where $a_0=\hbar^2/me^2$ is the Bohr radius,[5] and $n_s=N/S$ is the two-dimensional electron density. This r_s expansion is generated by a perturbative treatment of the Coulomb interaction similar to the one done in the 3D case. The Coulomb first-order term—also called the exchange energy—makes (as in 3D) an $R_0\ (r_s)^{-1}$ contribution, where $R_0=me^4/2\hbar^2$ is the Rydberg. The Coulomb second-order term stays finite, and makes a contribution in $R_0\ (r_s)^0$. At third order only, we start to find singular contributions generated by small momentum-transfer excitations which are similar to those appearing in the direct second-order term of the 3D case. Indeed, these small-q processes, which give rise to a $R_0 \ln r_s$ contribution in 3D, induce in 2D a logarithmic term starting in $R_0 r_s \ln r_s$ only.[2,3]

In the case of a quasi-2D electron gas, the finite width of the quantum well modifies the exact 2D results in two ways.

(i) First, the Coulomb matrix elements, associated with finite momentum-transfer excitations, appear as the exact 2D one $(2\pi e^2/q)$ multiplied by a form factor which depends on the well width.[6] This form factor modifies the contributions of the intrasubband transitions. It also, and mostly, allows intersubband transitions which generate additional contributions to the Coulomb energy: As the intersubband energy difference tends to infinity in the zero-well-width limit, these intersubband virtual excitations are negligible for very narrow wells and of course do not enter the exact 2D Coulomb energy. They appear at finite width only, and their contribution increases with the well width.

(ii) Second, the finite width induces Coulomb excitations with zero-momentum transfers. If taken alone, these $q=0$ Coulomb excitations give rise to the Hartree energy[7,8] already studied in a previous work.[9] When included in addition to $q\neq 0$ processes, these $q=0$ excitations generate additional mixed Hartree-exchange and Hartree-correlation terms to the usual small r_s expansion of the Coulomb energy.

In this paper, we study the effect of the $q\neq 0$ Coulomb form factor on the quasi-2D exchange[10–13] and correlation[12,14] energies. In addition to the usual direct and exchange second-order terms, we show that intersubband excitations generate an ''anomalous'' second-order term which does not exist in the $T=0$ exact 2D and 3D Coulomb energy. We also calculate the contributions of the mixed Hartree-exchange and Hartree-correlation terms to the Coulomb energy.

We will restrict ourselves here to densities large enough to have $r_s<1$ but low enough to have electrons in the lowest $n=1$ subband only. The existence of electrons in more than one subband raises additional difficulties due to the subband filling changes induced by the Coulomb interaction. These difficulties are beyond the scope of this paper and will be studied in a specific work.

For electrons in one subband only, we have

$$\varepsilon_1+\varepsilon_K<\varepsilon_2, \tag{2}$$

where ε_n is the free-electron localization energy, and ε_K is the 2D Fermi energy, $\varepsilon_K=\hbar^2K^2/2m$ with $K^2=2\pi N/S$. For a well of width a, with infinite barriers, $\varepsilon_n=\hbar^2\pi^2n^2/2ma^2$, so that Eq. (2) implies

$$\lambda=(2\pi)^{-1}Ka<\lambda_0=\sqrt{3}/2\simeq 0.866. \tag{3}$$

This dimensionless parameter λ turns out to be the appropriate one to measure the effect of a finite well width on the Coulomb energy. With the $(2\pi)^{-1}$ prefactor in the definition of λ, the coefficients of the λ expansion of this energy are found to be of the order of 1. Moreover, as λ remains smaller than 1 over the whole one-subband filling domain, the analytical expansions in λ of the various contributions to the Coulomb energy stay rather close to their exact values obtained numerically.

The paper is organized as follows. In Sec. I we recall the formalism of Refs. 9 and 12, and give the explicit expression of the form factor. In Sec. II we calculate the bare exchange energy and the first mixed Hartree-exchange contribution.

0163-1829/96/53(19)/12929(9)/$10.00

Section III is devoted to the correlation energy. We explicitly calculate the direct, exchange, and anomalous terms of the ‘‘bare’’ second-order correlation energy, and evaluate the mixed Hartree–second-order correlation terms.

I. COULOMB INTERACTION IN A QUASI-2D ELECTRON GAS

We consider a system made of N electrons localized in a quantum well and N ions inside or outside the well. Let $\varphi_{n\mathbf{k}}$ be the free electron wave functions in the well and $a^{+}_{n\mathbf{k}\sigma}$ the corresponding creation operators. In terms of these $a^{+}_{n\mathbf{k}\sigma}$, the free-electron Hamiltonian is diagonal and reads

$$\mathscr{H}_0=\sum_{n\mathbf{k}\sigma}(\varepsilon_n+\varepsilon_k)a^{+}_{n\mathbf{k}\sigma}a_{n\mathbf{k}\sigma}. \tag{4}$$

In the case of an infinite well located at $0<z<a$, $\varphi_{n\mathbf{k}}$ and the corresponding energies ε_n and ε_k are simply

$$\begin{gathered}\varphi_{n\mathbf{k}}(\boldsymbol{\rho},z)=\frac{e^{i\mathbf{k}\cdot\boldsymbol{\rho}}}{\sqrt{S}}\varphi_n(z),\quad \varphi_n(z)=\left(\frac{2}{a}\right)^{1/2}\sin\frac{n\pi z}{a},\\ \varepsilon_k=\frac{\hbar^2}{2m}k^2,\quad \varepsilon_n=\frac{\hbar^2}{2m}\frac{n^2\pi^2}{a^2}.\end{gathered} \tag{5}$$

In the following, explicit results will be given for infinite well barriers only, for which most of the calculations can be performed analytically. However, results for other types of wells can be formally obtained in the same way, by using the appropriate $\varphi_n(z)$ and ε_n for finite barriers.

In order to get rid of spurious divergences arising from the long-range character of the Coulomb forces, we consider the total Coulomb interaction of the N electron-ion system, i.e., the sum of the electron-electron, electron-ion *and ion-ion* interactions. Moreover, we will assume here that the dielectric constants are the same inside and outside the well. The effects induced by a dielectric constant difference and the image contributions it generates have been studied in Ref. 15, and are rather small in most cases.

We can divide the total Coulomb interaction into two parts corresponding to zero-momentum-transfer and finite-momentum-transfer excitations, respectively.

For an ion density $n_s\rho_i(z)$, the first part is given by[9]

$$\begin{aligned}\mathscr{V}^{(\mathbf{q}=\mathbf{0})}=\frac{1}{2}\frac{2\pi e^2}{Sa^{-1}}\sum_{\substack{n_1n_1'\\ n_2n_2'}}\sum_{\substack{\mathbf{k}_1\mathbf{k}_2\\ \sigma_1\sigma_2}}&W_{n_1n_1';n_2n_2'}a^{+}_{n_1\mathbf{k}_1\sigma_1}a^{+}_{n_2\mathbf{k}_2\sigma_2}\\ &\times a_{n_2'\mathbf{k}_2\sigma_2}a_{n_1'\mathbf{k}_1\sigma_1},\end{aligned} \tag{6}$$

$$\begin{aligned}W_{n_1n_1';n_2n_2'}=-\int\int dz_1\,dz_2\frac{|z_1-z_2|}{a}&[\varphi^{*}_{n_1}(z_1)\varphi_{n_1'}(z_1)\\ &-\rho_i(z_1)\delta_{n_1n_1'}][\varphi^{*}_{n_2}(z_2)\varphi_{n_2'}(z_2)-\rho_i(z_2)\delta_{n_2n_2'}].\end{aligned} \tag{7}$$

Explicit analytical expressions of the $W_{n_1n_1';n_2n_2'}$ are given in Ref. 9, for different ion configurations.

The Coulomb interaction with finite momentum transfers reads[12]

$$\begin{aligned}\mathscr{V}^{(\mathbf{q}\neq\mathbf{0})}=\frac{1}{2}\sum_{\mathbf{q}\neq 0}\frac{2\pi e^2}{Sq}\sum_{\substack{n_1n_1'n_2n_2'\\ \mathbf{k}_1\mathbf{k}_2\sigma_1\sigma_2}}&V_{n_1n_1';n_2n_2'}(aq/2\pi)a^{+}_{n_1\mathbf{k}_1+\mathbf{q}\sigma_1}\\ &\times a^{+}_{n_2\mathbf{k}_2-\mathbf{q}\sigma_2}a_{n_2'\mathbf{k}_2\sigma_2}a_{n_1'\mathbf{k}_1\sigma_1},\end{aligned} \tag{8}$$

where $V_{n_1n_1';n_2n_2'}$ is the form factor. It depends on the finite well width through $\varphi_n(z)$ but is independent of the ion configuration. It is precisely given by

$$\begin{aligned}V_{n_1n_1';n_2n_2'}(Q)=\int\int dz_1\,dz_2\,&e^{-2\pi Q|z_1-z_2|/a}\varphi^{*}_{n_1}(z_1)\\ &\times\varphi_{n_1'}(z_1)\varphi^{*}_{n_2}(z_2)\varphi_{n_2'}(z_2).\end{aligned} \tag{9}$$

In the $(Q=0)$ limit, the form factor is diagonal and reduces to $V_{n_1n_1';n_2n_2'}(0)=\delta_{n_1n_1'}\delta_{n_2n_2'}$; this corresponds to the exact 2D case, $a=0$, for which the Coulomb matrix element is simply $2\pi e^2/Sq$. For infinite well barriers, i.e., for $\varphi_n(z)$ given by Eq. (4), from Eq. (9) we obtain the following analytical expression of the form factor:

$$\begin{aligned}V_{n_1n_1';n_2n_2'}(Q)=G_0(Q)\delta_{n_1n_1'}\delta_{n_2n_2'}&+G_{n_1-n_1'}(Q)[\delta_{|n_1-n_1'|,|n_2-n_2'|}-\delta_{|n_1-n_1'|,n_2+n_2'}]+G_{n_1+n_1'}(Q)[\delta_{n_1+n_1',n_2+n_2'}-\delta_{n_1+n_1',|n_2-n_2'|}]\\ &-[1+(-1)^{n_1+n_1'+n_2+n_2'}][1-(-1)^{n_1+n_1'}e^{-2\pi Q}][G_{n_1-n_1'}(Q)-G_{n_1+n_1'}(Q)][G_{n_2-n_2'}(Q)-G_{n_2+n_2'}(Q)],\end{aligned} \tag{10}$$

$$G_n(Q)=2Q/\pi(4Q^2+n^2). \tag{11}$$

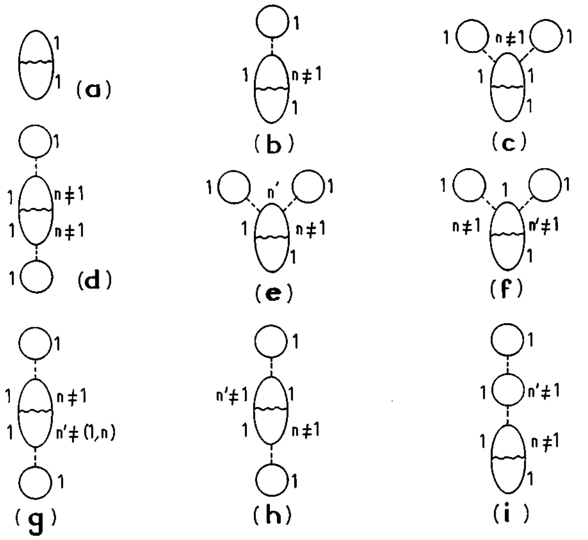

FIG. 1. Exchange diagrams: (a) ''bare'' term, i.e., without any Hartree process. (b) First mixed Hartree-exchange term, i.e., with one Hartree process. (c)–(i) Higher-order mixed Hartree-exchange terms. [Note that in (e) n' can be 1 as well.]

We can check that for small Q the form factor diagonal terms $V_{n_1n_1;n_2n_2}(Q)$ tend to 1, while the nondiagonal terms $V_{n_1n_1';n_2n_2'}(Q)$ (with $n_1 \neq n_1'$ and/or $n_2 \neq n_2'$) behave as Q.

The Coulomb energy of a quasi-2D electron gas is calculated as an expansion in $\mathcal{V}_{\text{coul}} = \mathcal{V}^{(\mathbf{q}=\mathbf{0})} + \mathcal{V}^{(\mathbf{q}\neq\mathbf{0})}$. The $\mathcal{V}^{(\mathbf{q}=\mathbf{0})}$ part of the Coulomb interaction, if take alone, generates the Hartree energy which has been calculated in Ref. 9. We have shown that the dimensionless parameter associated with the $\mathcal{V}^{(\mathbf{q}=\mathbf{0})}$ expansion is

$$\lambda_H = K^2 a^3/\pi^4 a_0 = (4\sqrt{2}/\pi) r_s \lambda^3, \tag{12}$$

which stays smaller than 1 for electrons in one subband only *and* for $r_s < 1$ (in order to perform an expansion in $\mathcal{V}^{(\mathbf{q}\neq\mathbf{0})}$). This explains why the Hartree energy is quite accurately given by the first plus possibly the second-order term of the $\mathcal{V}^{(\mathbf{q}=\mathbf{0})}$ expansion.

Here we study the other terms of the $(\mathcal{V}^{(\mathbf{q}=\mathbf{0})} + \mathcal{V}^{(\mathbf{q}\neq\mathbf{0})})$ expansion of the energy, i.e., the terms with at least one $\mathcal{V}^{(\mathbf{q}\neq\mathbf{0})}$.

II. EXCHANGE ENERGY

The exchange energy corresponds to all terms of the Coulomb expansion with one $\mathcal{V}^{(\mathbf{q}\neq\mathbf{0})}$, i.e., to terms in $\mathcal{V}^{(\mathbf{q}\neq\mathbf{0})})(\mathcal{V}^{(\mathbf{q}=\mathbf{0})})^p$ with $p \geq 0$.

A. ''Bare'' exchange energy

The ''bare'' exchange energy ($p=0$) corresponds to the diagram of Fig. 1(a). This term generates a contribution[12,13]

$$E_{x_0} = \langle 0 | \mathcal{V}^{(\mathbf{q}\neq\mathbf{0})} | 0 \rangle = -N R_0 r_s^{-1} A_x(\lambda). \tag{13}$$

We can transform the expression of $A_x(\lambda)$ given in Eq. (4) of Ref. 12 into

$$A_x(\lambda) = \frac{1}{\sqrt{2}\pi^2} \int \frac{d^2Q}{Q} J(Q) V_{11;11}(\lambda Q), \tag{14}$$

$$J(Q) = \int_{\substack{Q' \leq 1 \\ |\mathbf{Q}+\mathbf{Q}'| \leq 1}} d^2Q' = \begin{cases} 2\cos^{-1}\left(\dfrac{Q}{2}\right) - Q\left[1 - \dfrac{Q^2}{4}\right]^{1/2} & \text{for} \quad 0 \leq Q \leq 2 \\ 0 \quad \text{for} \quad Q \geq 2. \end{cases} \tag{15}$$

If $\lambda = 0$, $V_{11;11} = 1$ and $A_x(0) = 8\sqrt{2}/3\pi$, which is the exact 2D value of the exchange energy.[1] For small λ, we can expand $V_{11;11}$ and deduce the following expansion of $A_x(\lambda)$:

$$\begin{aligned} A_x(\lambda) = \sqrt{2}\biggl[& \frac{8}{3\pi} - \frac{4\pi^2 - 15}{12\pi}\lambda + \frac{64(\pi^2 - 6)}{135\pi}\lambda^2 \\ & - \frac{4\pi^4 - 40\pi^2 + 105}{60\pi}\lambda^3 \\ & + \frac{1024(2\pi^4 - 30\pi^2 + 135)}{23625\pi}\lambda^4 + O(\lambda^5)\biggr] \\ = {} & 1.200 - 0.918\lambda + 0.826\lambda^2 - 0.749\lambda^3 \\ & + 0.658\lambda^4 + O(\lambda^5). \end{aligned} \tag{16}$$

We can also calculate $A_x(\lambda)$ numerically by using the exact value of $V_{11;11}(Q)$. We find that the small-λ expansion of $A_x(\lambda)$ differs by less than 10% from its exact value at the maximum expected discrepancy, i.e., at the $(n=1, n=2)$ subband crossover $\lambda = \lambda_0$. Excellent agreement over the whole $0 \leq \lambda \leq \lambda_0$ range is obtained with the Padé approximant constructed from the first three terms of the $A_x(\lambda)$ expansion only, namely,

$$A_x(\lambda) \simeq \frac{1.200 + 0.361\lambda}{1 + 1.066\lambda + 0.124\lambda^2}. \tag{17}$$

As shown in Fig. 2, $A_x(\lambda)$ is a decreasing function of λ which varies from 1.200 to 0.750 for $0 \leq \lambda \leq \lambda_0$. This diminution, induced by the finite well width, is clearly significant.

B. Mixed Hartree-exchange energy

The first correction to this exchange energy, as induced by $q=0$ interactions, corresponds to the second-order mixed Hartree-exchange term [cf. Fig. 1(b)]. It is given by Eq. (15) of Ref. 12, and can be written as

$$E_{x_1} = N R_0 \lambda^4 B_x(\lambda), \tag{18}$$

where

$$B_x(\lambda) = \frac{32}{\pi} \sum_{n>1} \frac{W_{11;1n}}{n^2 - 1} \int \frac{d^2Q}{\lambda Q} J(Q) V_{11;1n}(\lambda Q) \tag{19}$$

stays finite when $\lambda \to 0$.

We find that the mixed Hartree-exchange energy E_{x_1} is $r_s \lambda^4$ smaller than the bare exchange energy E_{x_0}. A factor

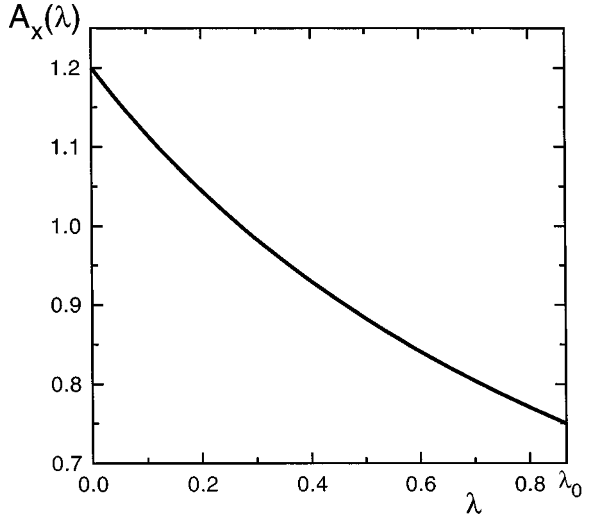

FIG. 2. ''Bare'' exchange energy coefficient $A_x(\lambda)$, defined in Eq. (13), as a function of the density through λ defined in Eq. (3).

$(e^2a)\propto(r_s\lambda)$ comes from the $\mathscr{V}^{(\mathbf{q}=\mathbf{0})}$ interaction, another factor $(a)^2\propto\lambda^2$ comes from the energy difference between states $\varphi_{1\mathbf{k}}$ and $\varphi_{n\mathbf{k}}$ coupled by the $\mathscr{V}^{(\mathbf{q}=\mathbf{0})}$ interaction, while an additional λ factor comes from the $V_{11;1n}(\lambda Q)$ matrix element which cancels as λ when $\lambda\to0$.

As $W_{11;1n}$ depends on the ion density $\rho_i(z)$, different ion configurations are expected to give different $B_x(\lambda)$. However, as shown in Ref. 1, all configurations with ions outside the electron layer give the same $W_{11;1n}$ so that they give the same $B_x(\lambda)$. Conversely, when ions are inside the well, $B_x(\lambda)$ depends on the precise ion configuration.

Using the small-Q limit of $V_{11;1n}(Q)$, we can calculate the small-λ limit of $B_x(\lambda)$. For ions outside the electron layer we find

$$B_x^{(\mathrm{out})}(0)=\frac{20}{3}-\frac{54}{\pi^2}-\frac{4\pi^2}{45}\simeq0.318, \tag{20}$$

while for ions *evenly distributed* inside the well, we find

$$B_x^{(\mathrm{in})}(0)=\frac{5}{4\pi^2}\simeq0.127. \tag{21}$$

At the $(n=1,n=2)$ subband crossover, numerical calculations show that $B_x(\lambda)$ is reduced by a factor of 3 $[B_x^{(\mathrm{out})}(\lambda_0)\simeq0.107$, while $B_x^{(\mathrm{in})}(\lambda_0)\simeq0.043]$. Excellent fits of $B_x(\lambda)$ over the $0\leqslant\lambda\leqslant\lambda_0$ range are given by

$$B_x^{(\mathrm{out})}(\lambda)\simeq\frac{0.318+0.040\lambda}{1+1.838\lambda+0.929\lambda^2}, \tag{22}$$

$$B_x^{(\mathrm{in})}(\lambda)\simeq\frac{0.127+0.016\lambda}{1+1.832\lambda+0.924\lambda^2}. \tag{23}$$

C. Higher-order terms

The exchange energy terms with two $\mathscr{V}^{(\mathbf{q}=\mathbf{0})}$ interactions correspond to the diagrams shown on Figs. 1(c)–1(i). The dominant ones for small λ [Figs. 1(c) and 1(d)] contain a diagonal matrix element ($V_{11;11}$ or $V_{11;nn}$) and can be shown to be in $r_s\lambda^6$ in the small-λ limit. The other diagrams contain a nondiagonal matrix element $V_{11;1n}$ or $V_{1n;1n'}$ and are thus λ smaller, i.e., in $r_s\lambda^7$.

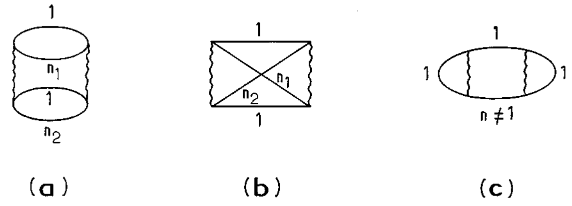

FIG. 3. ''Bare'' second-order correlation diagrams. In (a) and (b), n can be equal to 1, while in (c) n must differ from 1 in order to make a nonzero contribution.

As these second-order Hartree-exchange terms are all in $(r_s)^1$, they do not enter the second-order r_s expansion of the exchange energy, which thus reads

$$\frac{E_x}{NR_0}=\varepsilon_x=-\frac{1}{r_s}A_x(\lambda)+\lambda^4B_x(\lambda)+O(r_s). \tag{24}$$

III. CORRELATION ENERGY

The correlation energy corresponds to all terms of the Coulomb expansion of the energy with two $\mathscr{V}^{(\mathbf{q}\neq\mathbf{0})}$ at least, i.e., to terms in $(\mathscr{V}^{(\mathbf{q}\neq\mathbf{0})})^m\ (\mathscr{V}^{(\mathbf{q}=\mathbf{0})})^p$ with $m\geqslant2$ and $p\geqslant0$. We concentrate here on the second-order term, i.e., $m=2$.

A. ''Bare'' second-order correlation energy

The leading contribution to the correlation energy comes from the term with two $\mathscr{V}^{(\mathbf{q}\neq\mathbf{0})}$ only. The associated diagrams are shown in Figs. 3(a)–3(c). The first two are the usual direct and exchange diagrams analogous to those appearing in the second-order term of the 3D correlation energy. The third one does not appear in the usual diagrammatic expansion of the 3D correlation energy since it cancels at $T=0$. However, this ''anomalous'' term does not cancel in quasi-2D systems, due to the possibility of intersubband transitions.

1. Direct and exchange terms

For a $|0\rangle$ state with electrons in the $n=1$ subband only, the usual direct and exchange terms [cf. Figs. 3(a) and 3(b)] read[12]

$$E_c^{(d+e)}=\left(\frac{2\pi e^2}{S}\right)^2\sum_{\mathbf{q}\neq\mathbf{0}}\sum_{\substack{n_1n_2\\ \mathbf{k}_1\mathbf{k}_2}}\left[\frac{2V^2_{1n_1;1n_2}(\lambda q/K)}{q^2}-\frac{V_{1n_1;1n_2}(\lambda q/K)V_{1n_1;1n_2}(\lambda|\mathbf{q}+\mathbf{k}_1-\mathbf{k}_2|/K)}{q|\mathbf{q}+\mathbf{k}_1-\mathbf{k}_2|}\right]\times\frac{f_{\mathbf{k}_1}(1-\delta_{1,n_1}f_{\mathbf{k}_1+\mathbf{q}})f_{\mathbf{k}_2}(1-\delta_{1,n_2}f_{\mathbf{k}_2-\mathbf{q}})}{2\varepsilon_1-\varepsilon_{n_1}-\varepsilon_{n_2}+\varepsilon_{\mathbf{k}_1}+\varepsilon_{\mathbf{k}_2}-\varepsilon_{\mathbf{k}_1+\mathbf{q}}-\varepsilon_{\mathbf{k}_2-\mathbf{q}}}, \tag{25}$$

where $f_{\mathbf{k}}=\theta(K-|\mathbf{k}|)$ is the $T=0$ Fermi distribution. Because of the existence of intersubband transitions induced by the finite well width, we have to consider intrasubband $(n_1=n_2=1)$ as well as intersubband $(n_1\neq 1, n_2\neq 1)$ and intersubband-intrasubband $(n_1\neq 1=n_2$ or $n_2\neq 1=n_1)$ processes. Let us consider their contributions separately.

(i) (1→1,1→1) transitions. We first note that, since $V_{1n_1;1n_2}(0)=\delta_{1,n_1}\delta_{1,n_2}$, these transitions are the only ones appearing in the exact 2D limit ($a=0$ or, equivalently, $\lambda=0$). For a finite width they give

$$E_c^{(\mathrm{intra})}(\lambda)=-NR_0 B_c^{(\mathrm{intra})}(\lambda), \tag{26}$$

$$B_c^{(\mathrm{intra})}(\lambda)=\frac{1}{4\pi^3}\int_{\substack{Q_1\leqslant 1\leqslant|\mathbf{Q}_1+\mathbf{Q}|\\ Q_2\leqslant 1\leqslant|\mathbf{Q}_2-\mathbf{Q}|}}\int\int\frac{d^2Q\ d^2Q_1\ d^2Q_2}{\mathbf{Q}\cdot(\mathbf{Q}+\mathbf{Q}_1-\mathbf{Q}_2)}\times\left[\frac{2V_{11;11}^2(\lambda Q)}{Q^2}-\frac{V_{11;11}(\lambda Q)V_{11;11}(\lambda|\mathbf{Q}+\mathbf{Q}_1-\mathbf{Q}_2|)}{Q|\mathbf{Q}+\mathbf{Q}_1-\mathbf{Q}_2|}\right]. \tag{27}$$

For $\lambda=0$, we recover the leading term of the exact 2D correlation energy,[2–4] as expected. For small λ, we can expand $V_{11;11}(\lambda Q)$ and, from it, deduce the analytical expansion of $B_c^{(\mathrm{intra})}(\lambda)$. Singular contributions, coming from $Q\sim\lambda^{-1}$, appear at second order, leading to a $(\lambda^2\ln\lambda)$ term. The first terms of the $B_c^{(\mathrm{intra})}(\lambda)$ expansion are

$$\begin{aligned}B_c^{(\mathrm{intra})}(\lambda)&=2(1-\ln 2)-0.229-\frac{4(\pi-2)(4\pi^2-15)}{9\pi^2}\lambda\\&\quad-\frac{40\pi^4-264\pi^2+225}{72\pi^2}\lambda^2\ln\lambda+O(\lambda^2)\\&=0.385-1.258\lambda-2.133\lambda^2\ln\lambda+O(\lambda^2).\end{aligned} \tag{28}$$

We can also calculate $B_c^{(\mathrm{intra})}(\lambda)$ numerically. The direct term can be reduced to a first-order integral by using

$$\int_{Q_1\leqslant 1\leqslant|\mathbf{Q}_1+\mathbf{Q}|}d^2Q_1\int_{Q_2\leqslant 1\leqslant|\mathbf{Q}_2-\mathbf{Q}|}d^2Q_2\,\frac{1}{\mathbf{Q}_1\cdot(\mathbf{Q}+\mathbf{Q}_1-\mathbf{Q}_2)}=2\pi Q\,\psi\left(\frac{Q}{2}\right),$$

$$\psi(0\leqslant x\leqslant 1)=\sqrt{1-x^2}+\frac{1}{x}\sin^{-1}(x)-\frac{2}{3x^2}\times[(x^2+1)\mathbf{E}(x)+(x^2-1)\mathbf{K}(x)], \tag{29}$$

$$\psi(1\leqslant x)=\frac{\pi}{2x}-\frac{2}{3x}\left[(x^2+1)\mathbf{E}\left(\frac{1}{x}\right)+(1-x^2)\mathbf{K}\left(\frac{1}{x}\right)\right],$$

where $\mathbf{K}(x)$ and $\mathbf{E}(x)$ are the complete elliptic integrals of the first and second kinds. The exchange term has been calculated as a quintuple integral. The resulting $B_c^{(\mathrm{intra})}(\lambda)$ can be fitted over the whole density range $0\leqslant\lambda\leqslant\lambda_0$ by the following expression:

$$B_c^{(\mathrm{intra})}(\lambda)\simeq\frac{0.385+2.185\lambda}{1+8.767\lambda+13.11\lambda^2}. \tag{30}$$

$B_c^{(\mathrm{intra})}(\lambda)$ decreases from 0.385 to 0.124 when λ increases from 0 to λ_0.

(ii) (1→1,1→n≠1) transitions. The contribution to the correlation energy coming from processes in which one electron is excited outside the lowest subband cancels with the well width. Indeed, as $V_{11;1n}(\lambda Q)$ behaves as λQ in the small-λ limit, this contribution must cancel as λ^2. Moreover, as $V_{11;1n}=0$ for even values of n, the electron excited outside the $n=1$ subband can only reach subbands with odd parity. From Eq. (25), we precisely find

$$E_c^{(\mathrm{inter1})}(\lambda)=-NR_0\lambda^2 b_c^{(1)}(\lambda), \tag{31}$$

$$b_c^{(1)}(\lambda)=\frac{4}{\pi^3}\sum_{n\geqslant 3}\int\int\frac{d^2Q\ d^2Q'}{n^2-1+8\lambda^2\mathbf{Q}\cdot\mathbf{Q}'}I_1(\mathbf{Q},\mathbf{Q}')\times\left[\frac{2V_{11;1n}^2(\lambda Q)}{Q^2}-\frac{V_{11;1n}(\lambda Q)V_{11;1n}(\lambda Q')}{QQ'}\right], \tag{32}$$

where

$$I_1(\mathbf{Q},\mathbf{Q}')=\int_{\substack{Q''\leqslant 1\leqslant|\mathbf{Q}''+\mathbf{Q}|\\ |\mathbf{Q}''+\mathbf{Q}-\mathbf{Q}'|\leqslant 1}}d^2Q''=\int_{\substack{P\geqslant 1\\ |\mathbf{P}-\mathbf{Q}|,|\mathbf{P}-\mathbf{Q}'|\leqslant 1}}d^2P \tag{33}$$

is the area inside two circles and outside a third one. The analytical expression of $I_1(\mathbf{Q},\mathbf{Q}')$ is given in the Appendix. From Eq. (32), it is not obvious that $b_c^{(1)}(0)$ is finite. Nevertheless, by setting $\lambda\mathbf{Q}=\mathbf{Q}_1$ and $\mathbf{Q}'=\mathbf{Q}+\mathbf{Q}_2$, we find

$$b_c^{(1)}(0)=\frac{4}{\pi}\sum_{n\geqslant 3}\int d^2Q_1\frac{V_{11;1n}^2(Q_1)}{Q_1^2(n^2-1+8Q_1^2)}\simeq 0.0115. \tag{34}$$

$b_c^{(1)}(\lambda)$ can be calculated as a triple integral. For $0\leqslant\lambda\leqslant\lambda_0$, it decreases from 0.0115 to 0.0052. Excellent agreement with numerically obtained values of $b_c^{(1)}(\lambda)$ is provided by

$$b_c^{(1)}(\lambda)\simeq\frac{0.0115+0.0909\lambda^2}{1+12.51\lambda^2+9.185\lambda^4}. \tag{35}$$

(iii) (1→n₁≠1,1→n₂≠1) transitions. Turning to processes in which the two electrons are excited outside the lowest subband, we first note that the corresponding contribution to the correlation energy also cancels as λ^2 with the well width. Moreover, since $V_{1n_1;1n_2}=0$ for odd values of (n_2-n_1), the two electrons can only reach subbands of the same parity. From Eq. (25) we precisely find

$$E_c^{(\mathrm{inter2})}(\lambda)=-NR_0\lambda^2 b_c^{(2)}(\lambda), \tag{36}$$

$$b_c^{(2)}(\lambda)=\frac{2}{\pi^3}\sum_{n_1\geqslant 2}\sum_{n_2\geqslant 2}\int\int\frac{d^2Q_1\,d^2Q_2}{n_1^2+n_2^2-2+8\mathbf{Q}_1\cdot(\mathbf{Q}_1+\lambda\mathbf{Q}_2)}\times J(Q_2)\left[\frac{2V_{1n_1;1n_2}^2(Q_1)}{Q_1^2}-\frac{V_{1n_1;1n_2}(Q_1)V_{1n_1;1n_2}(|\mathbf{Q}_1+\lambda\mathbf{Q}_2|)}{Q_1|\mathbf{Q}_1+\lambda\mathbf{Q}_2|}\right], \tag{37}$$

where $J(Q)$ is given by Eq. (15). For $0\leqslant\lambda\leqslant\lambda_0$, $b_c^{(2)}$ increases from 0.0316 to 0.0397, and can be fitted by the following expression:

$$b_c^{(2)}(\lambda)\simeq\frac{0.0316+0.167\lambda^2+0.0445\lambda^4}{1+4.798\lambda^2}. \tag{38}$$

(iv) Direct and exchange second-order correlation energy. Summing intrasubband and intersubband contributions, we obtain

$$E_c^{(d+e)}=-NR_0[B_c^{(\text{intra})}(\lambda)+\lambda^2B_c^{(\text{inter})}(\lambda)], \tag{39}$$

$$B_c^{(\text{inter})}(\lambda)=b_c^{(1)}(\lambda)+b_c^{(2)}(\lambda).$$

The intrasubband contribution $B_c^{(\text{intra})}(\lambda)$ decreases from 0.385 to 0.124 when λ increases from 0 to λ_0, while the intersubband contribution $\lambda^2B_c^{(\text{inter})}(\lambda)$ increases from 0 to 0.0337 and thus remains small when compared to the intrasubband term.

2. Anomalous exchange term

The ''anomalous'' exchange term, corresponding to the diagram of Fig. 3(c), does not cancel at $T=0$ in quasi-2D systems, because of the existence of intersubband processes induced by the finite well width. This term, given by Eq. (18) of Ref. 12, cancels with the well width as λ^4 [a λ^2 factor comes from the small-λ value of the two $V_{11;1n}$, and an additional λ^2 comes from the energy denominator $(\varepsilon_1-\varepsilon_n)$]. We precisely find

$$E_c^{(a)}=-NR_0\lambda^4B_c^{(a)}(\lambda), \tag{40}$$

$$B_c^{(a)}(\lambda)=\frac{4}{\pi^3\lambda^2}\sum_{n\geqslant 3}\frac{1}{n^2-1}\int\int d^2Q\,d^2Q'\,I_2(\mathbf{Q},\mathbf{Q}')\times\frac{V_{11;1n}(\lambda Q)V_{11;1n}(\lambda Q')}{QQ'}, \tag{41}$$

where

$$I_2(\mathbf{Q},\mathbf{Q}')=\int_{P,|\mathbf{P}-\mathbf{Q}|,|\mathbf{P}-\mathbf{Q}'|\leqslant 1}d^2P \tag{42}$$

is the area inside three circles. The analytical expression of $I_2(\mathbf{Q},\mathbf{Q}')$ is given in the Appendix.

The $\lambda=0$ limit of $B_c^{(a)}$ is easily obtained from the small-q limit of $V_{11;1n}(q)$. We find

$$B_c^{(a)}(0)=\frac{5}{3}-\frac{27}{2\pi^2}-\frac{\pi^2}{45}\simeq 0.0795. \tag{43}$$

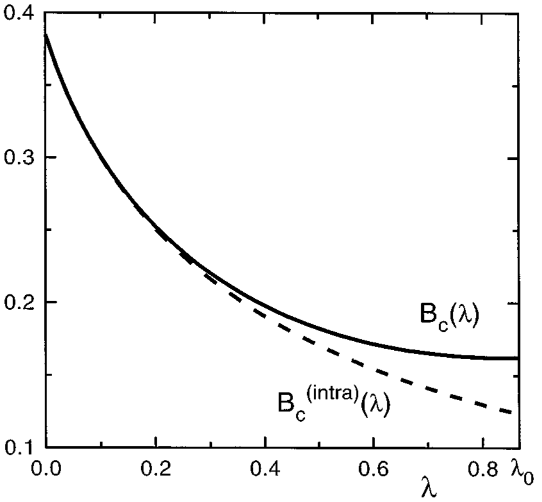

FIG. 4. ''Bare'' second-order correlation energy in Rydberg units, as a function of λ. At small λ, the dominant contribution $B_c^{(\text{intra})}(\lambda)$ comes from intrasubband processes, i.e., from $n_1=n_2=1$ in Figs. 3(a) and 3(b).

From Eq. (41), $B_c^{(a)}(\lambda)$ is obtained as a sum of triple integrals. For $0\leqslant\lambda\leqslant\lambda_0$, it decreases from 0.0795 to 0.0092. A fit of $B_c^{(a)}(\lambda)$ can be obtained by

$$B_c^{(a)}(\lambda)\simeq\frac{0.0795-0.0249\lambda}{1+3.079\lambda+3.550\lambda^2}. \tag{44}$$

The anomalous contribution to the second-order correlation energy $\lambda^4B_c^{(a)}(\lambda)$ increases with λ from 0 to 0.005 (for $\lambda=\lambda_0$), and is thus almost negligible with respect to the direct and exchange terms.

3. ''Bare'' second-order correlation energy

The well-width dependence of the correlation term with two $V^{(q\neq 0)}$ only is given by

$$E_c^{(2)}=-NR_0[B_c^{(\text{intra})}(\lambda)+\lambda^2B_c^{(\text{inter})}(\lambda)+\lambda^4B_c^{(a)}(\lambda)]=-NR_0B_c(\lambda). \tag{45}$$

When λ increases from 0 to λ_0, $B_c(\lambda)$ decreases from its exact 2D value 0.385 to 0.162. The ''bare'' correlation energy (like the exchange energy) of a quasi-2D system is always smaller than the exact 2D one, the diminution being significant for usual well widths.

In Fig. 4 we plot $B_c(\lambda)$ and the intrasubband contribution $B_c^{(\text{intra})}(\lambda)$. These two curves are in fact rather close, the λ dependence of the ''bare'' second-order correlation energy being dominated by direct and exchange intrasubband processes. The intersubband contribution to the direct and exchange terms plus the anomalous term tend to compensate for the decrease of the intrasubband term, but this compensation is only partial.

B. Mixed Hartree–second-order correlation energy

If we now consider terms with two $\mathcal{V}^{(\mathbf{q}\neq\mathbf{0})}$ and one $\mathcal{V}^{(\mathbf{q}=\mathbf{0})}$ at least, we generate the mixed Hartree–second-order correlation energy terms. The leading ones contain *one*

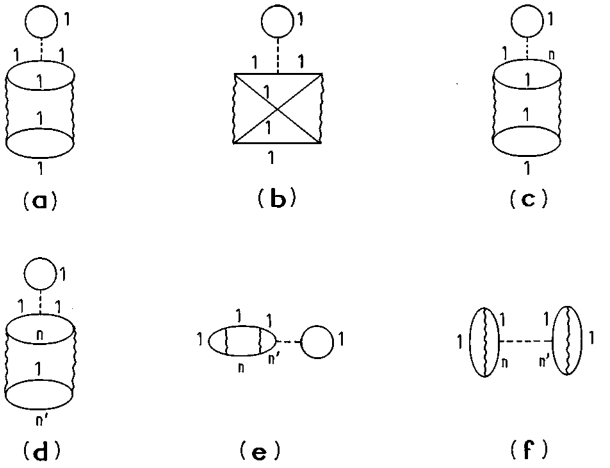

FIG. 5. Mixed Hartree–second-order correlation diagrams. The intersubband diagrams (c)–(f), in which all n differ from 1, make contributions of higher order in λ than the intrasubband diagrams (a) and (b). Besides diagram (f), they all come from adding a ''tadpole'' to the bare second-order diagrams.

$\mathscr{V}^{(\mathbf{q}=\mathbf{0})}$ only. A simple way to construct the corresponding diagrams is to add one ''tadpole'' to the bare second-order diagrams of Fig. 3. All these terms are *a priori* $(e^2a)\sim(r_s\lambda)$ smaller than the bare correlation energy, due to the additional $\mathscr{V}^{(\mathbf{q}=\mathbf{0})}$ matrix element, with possible extra factors λ coming from intersubband processes. We do find that the intrasubband diagrams of Figs. 5(a) and 5(b) are in $(r_s\lambda)$, while all other ones [Figs. 5(c), 5(d), and 5(e)] are of higher order in λ. If we consider the particular diagram of Fig. 5(e), we find that for small λ the corresponding term is in $r_s\lambda^7$ [with λ^4 coming from the bare diagram of Fig. 3(c), $(r_s\lambda)$ coming from the $\mathscr{V}^{(\mathbf{q}=\mathbf{0})}$ matrix element, and λ^2 coming from the energy denominator of the $(1\rightarrow n')$ intersubband excitation].

There are in fact other types of mixed Hartree-correlation diagrams in which the additional $\mathscr{V}^{(\mathbf{q}=\mathbf{0})}$ are not associated with ''tadpoles.'' One of them is shown in Fig. 5(f): Here the $\mathscr{V}^{(\mathbf{q}=\mathbf{0})}$ interaction is used to link two exchange diagrams. We can show that in the small-λ limit, the corresponding term behaves as $r_s\lambda^7$.

If we want to include all the terms in $(\mathscr{V}^{(\mathbf{q}\neq\mathbf{0})})^2\ \mathscr{V}^{(\mathbf{q}=\mathbf{0})}$ in the correlation energy, it is necessary to compare them with the ''bare'' third-order correlation terms in $(\mathscr{V}^{(\mathbf{q}\neq\mathbf{0})})^3$. Some of them are shown in Fig. 6. All being in $(e^2)^3$, they are *a priori* of the same order in r_s. Among them, the ring diagram of Fig. 6(a) is in fact singular in the small-q limit. By summing all ring diagrams with three or more $\mathscr{V}^{(\mathbf{q}\neq\mathbf{0})}$ interactions, we get rid of their singularities and generate a term in $(r_s\ln r_s)$ analogous to the one which appears in the r_s expansion of the exact 2D correlation energy.

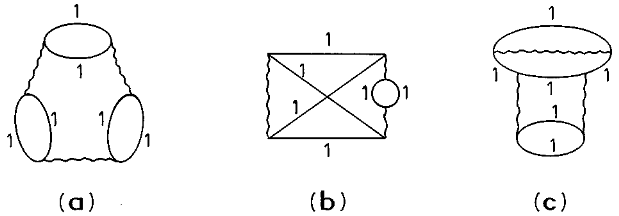

FIG. 6. A few ''bare'' third-order correlation diagrams.

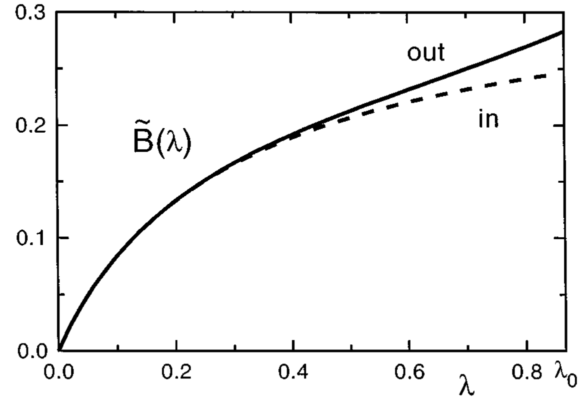

FIG. 7. Correction $\widetilde{B}(\lambda)$ to the exact 2D correlation energy, defined in Eq. (48), as a function of the density.

We thus conclude that, if we want to consider more terms in the small-r_s expansion of the quasi-2D correlation energy than the one of Eq. (45), we must first include the intrasubband ring diagrams which make a $(r_s\ln r_s)$ contribution. Next, we must add the other third-order intrasubband diagrams, such as those in Figs. 6(b) and 6(c), which are in r_s; only then can we consider the intrasubband mixed Hartree–second-order correlation terms [Figs. 5(a) and 5(b)] which are in $(r_s\lambda)$.

IV. COULOMB ENERGY TO SECOND ORDER IN r_s

From the above results we can deduce the part of the Coulomb energy of a quasi-2D electron gas which is induced by finite-momentum-transfer excitations, up to second order in r_s. We find[16]

$$\begin{aligned}E_{\text{coul}}^{(q\neq0)}&=E_x+E_c\\&=NR_0\left[\frac{1}{r_s}[-1.200+\widetilde{A}(\lambda)]\right.\\&\qquad\left.+[-0.385+\widetilde{B}(\lambda)]+O(r_s\ln r_s)\right],\end{aligned}\tag{46}$$

where $\widetilde{A}(\lambda)$ and $\widetilde{B}(\lambda)$ are the corrections to the exact 2D exchange and correlation energies. They are given by

$$\widetilde{A}(\lambda)=A_x(0)-A_x(\lambda),\tag{47}$$

$$\begin{aligned}\widetilde{B}(\lambda)=B_c^{(\text{intra})}(0)-[B_c^{(\text{intra})}(\lambda)+\lambda^2B_c^{(\text{inter})}(\lambda)\\+\lambda^4B_c^{(a)}(\lambda)]+\lambda^4B_x(\lambda),\end{aligned}\tag{48}$$

where $A_x(\lambda)$ is given by Eq. (14) and shown in Fig. 2. Note that $\widetilde{B}(\lambda)$ contains the finite width effect on the dominant term of the correlation energy as well as the contribution of the first mixed Hartree-exchange term. The well-width dependence of $\widetilde{B}(\lambda)$ is shown in Fig. 7.

It can be interesting and useful to compare the $(q\neq0)$ corrections to the exact 2D Coulomb energy with the Hartree energy.[9] The Hartree energy, as induced by the $\mathscr{V}^{(\mathbf{q}=\mathbf{0})}$ part of the Coulomb interaction, comes from the charge separation between electrons and ions. This charge separation reduces to zero in the zero-well-width limit,[17] so that the Hartree energy can also been seen as a well-width correction to the exact 2D Coulomb energy. Using Ref. 9, we find that the $\mathscr{V}^{(\mathbf{q}=\mathbf{0})}$ expansion of this Hartree energy can be written in the form

$$E_H = NR_0\left[\frac{1}{r_s}a_H\lambda - \lambda^4 b_H + O(r_s)\right], \tag{49}$$

so that the total Coulomb energy reads[12]

$$E_H + E_{\text{coul}}^{(q\neq 0)} = NR_0\left\{\frac{1}{r_s}[-1.200 + A(\lambda)] + [-0.385 + B(\lambda)] + O(r_s \ln r_s)\right\}. \tag{50}$$

$A(\lambda)$ and $B(\lambda)$ are shown in Ref. 12. The largest contribution to $A(\lambda)$ comes from the electrostatic energy necessary to separate the electrons from the ions. $A(\lambda)$ is thus much larger for ions outside the electron layer than for ions inside. Besides this naive electrostatic term, the rest of the Hartree part of $A(\lambda)$, coming from the deformation of the electron wave functions in the well, is of the order of the effect of the form factor on the exchange energy measured by $\widetilde{A}(\lambda)$.

Turning to $B(\lambda)$, we find that its small-λ behavior is always dominated by *intrasubband* direct and exchange-correlation energies, while at larger densities the result strongly depends on the ion configuration. Indeed, for densities close to the two-subband filling threshold *and* for ions on one side of the electron layer, the Hartree part is large and controls $B(\lambda)$. Conversely, for ions inside the well, the intrasubband correlation term still dominates.

V. CONCLUSION

We have calculated the exchange energy and the second-order correlation energy of a $T=0$ quasi-2D electron gas, taking into account the finite width of the well. This finite width generates a form factor which modifies the $(q\neq 0)$ Coulomb interaction and, in particular, allows intersubband excitations. It also yields a $(q=0)$ Coulomb interaction and thus generates mixed Hartree-exchange and Hartree-correlation terms which come from mixed $(q=0, q\neq 0)$ processes.

We show that for electrons in the lowest subband only, these exchange and correlation energies can be reduced by a factor of the order of 2 when compared with their exact 2D value.

APPENDIX: I_1 AND I_2 INTEGRALS

The integral $I_1(\mathbf{q},\mathbf{q}')$ defined in Eq. (33) represents the area inside two circles centered at $\mathbf{q}$ and $\mathbf{q}'$ and outside a third circle centered at the origin 0, all circles having a radius equal to 1. The integral $I_2(\mathbf{q},\mathbf{q}')$ defined in Eq. (42) represents the area inside the same three circles. These areas can be expressed as functions of q, q', and the angle θ between $\mathbf{q}$ and $\mathbf{q}'$ $(0\leqslant\theta\leqslant\pi)$.

Let us set

$$\alpha_1 = \cos^{-1}\left(\frac{q'}{2}\right), \quad \alpha_2 = \cos^{-1}\left(\frac{q}{2}\right),$$

$$\alpha_3 = \cos^{-1}\left[\frac{(q^2+q'^2-2qq'\cos\theta)^{1/2}}{2}\right], \tag{A1}$$

$$\theta_1 = \cos^{-1}\left[\frac{q-q'\cos\theta}{(q^2+q'^2-2qq'\cos\theta)^{1/2}}\right],$$

$$\theta_2 = \cos^{-1}\left[\frac{q'-q\cos\theta}{(q^2+q'^2-2qq'\cos\theta)^{1/2}}\right], \tag{A2}$$

$$\beta = \cos^{-1}\left[\frac{q^2+q'^2-4}{2qq'}\right],$$

$$\varphi(x) = \tfrac{1}{2}(x-\sin x), \tag{A3}$$

$$f(x,y,z) = \tfrac{1}{4}[2(x^2y^2+y^2z^2+z^2x^2)-(x^4+y^4+z^4)]^{1/2}, \tag{A4}$$

$$K(\mathbf{q},\mathbf{q}') = f\left[2\sin\left(\frac{\alpha_1+\alpha_2-\theta}{2}\right), 2\sin\left(\frac{\alpha_1+\alpha_3-\theta_2}{2}\right), 2\sin\left(\frac{\alpha_2+\alpha_3-\theta_1}{2}\right)\right] + \varphi(\alpha_1+\alpha_2-\theta) + \varphi(\alpha_1+\alpha_3-\theta_2) + \varphi(\alpha_2+\alpha_3-\theta_1). \tag{A5}$$

By considering the various geometrical configurations corresponding to the possible relative positions of the three circles, we find the following results:

$$I_2 = 2\varphi(2\alpha_1) \quad \text{for } q\leqslant q'\leqslant 2 \quad \text{and } 0\leqslant\theta\leqslant\alpha_2-\alpha_1, \tag{A6}$$

$$I_2 = 2\varphi(2\alpha_2) \quad \text{for } q'\leqslant q\leqslant 2 \quad \text{and } 0\leqslant\theta\leqslant\alpha_1-\alpha_2, \tag{A7}$$

$$I_2 = K(q,q') \quad \text{for } q,q'\leqslant 2 \quad \text{and } |\alpha_1-\alpha_2|\leqslant\theta\leqslant\alpha_1+\alpha_2, \tag{A8}$$

$$I_2 = 2\varphi(2\alpha_3) \quad \text{for } q+q'\leqslant 2 \quad \text{and } \alpha_1+\alpha_2\leqslant\theta\leqslant\pi, \tag{A9}$$

$$I_2 = 2\varphi(2\alpha_3) \quad \text{for } 0\leqslant 2-q\leqslant q'\leqslant\sqrt{4-q^2} \quad \text{and } \alpha_1+\alpha_2\leqslant\theta\leqslant\beta, \tag{A10}$$

$$I_2 = 0 \quad \text{for } q,q'\leqslant 2 \text{ with } q^2+q'^2\geqslant 4 \quad \text{and } \alpha_1+\alpha_2\leqslant\theta\leqslant\beta, \tag{A11}$$

$$I_2 = 0 \quad \text{for } |q-q'|\leqslant 2 \quad \text{and } 0\leqslant\theta\leqslant\beta. \tag{A12}$$

For the configurations corresponding to Eqs. (A6) to (A12), we have

$$I_1 = 2\varphi(2\alpha_3) - I_2. \tag{A13}$$

For all other values of q, q', and θ, I_1 and I_2 are equal to zero.

[1] F. Stern, Phys. Rev. Lett. **30**, 278 (1973).

[2] A. K. Rajagopal and J. C. Kimball, Phys. Rev. B **15**, 2819 (1977).

[3] A. Isihara and T. Toyoda, Ann. Phys. (N.Y.) **106**, 394 (1977).

[4] A. Isihara and L. C. Ioriatti, Jr., Phys. Rev. B **22**, 214 (1980).

[5] We have set $e^2=q^2/4\pi\varepsilon_0\varepsilon$, where q is the electron charge and ε the dielectric constant of the material. Here we assume that this dielectric constant is the same inside and outside the quantum well.

[6] T. Ando, A. B. Fowler, and F. Stern, Rev. Mod. Phys. **54**, 437 (1982).

[7] N. Ashcroft and D. Mermin, *Solid State Physics* (Saunders, Philadelphia, 1976), p. 330.

[8] A. Fetter and J. Walecka, *Quantum Theory of Many-Particle Systems* (McGraw-Hill, New York, 1971), p. 121.

[9] M. Combescot, O. Betbeder-Matibet, C. Benoit a la Guillaume, and K. Boujdaria, Solid State Commun. **88**, 309 (1993).

[10] K. M. S. V. Bandara, D. D. Coon, O. Byungsung, Y. F. Lin, and M. H. Francombe, Appl. Phys. Lett. **53**, 1931 (1988).

[11] M. L. Glasser, F. Garcia-Moliner, and V. R. Velasco, Phys. Scr. **43**, 512 (1991).

[12] O. Betbeder-Matibet, M. Combescot, and C. Tanguy, Phys. Rev. Lett. **72**, 4125 (1994).

[13] H. Totsuji, H. Tachibana, C. Totsuji, and S. Nara, Phys. Rev. B **51**, 11 148 (1995).

[14] J. C. Ryan and T. L. Reinecke, Phys. Rev. B **47**, 9615 (1993).

[15] O. Betbeder-Matibet and M. Combescot, Solid State Commun. **94**, 221 (1995).

[16] When electrons occupy more than one subband, exchange and correlation energies are *not* given by Eq. (45). Specific problems arise in this case, which will be studied in a forthcoming publication.

[17] This is clearly true for ions inside the well, and remains true for ions outside the well, in the configurations considered in Ref. 9, i.e., for ions located at $-a<z<0$ (or located at $-a/2<z<0$ and $a<z<3a/2$). Nevertheless, for such ‘‘out’’ configurations, the spirit of a zero well width limit would rather correspond to electrons located in the $z=a/2$ plane and ions located in the $z=-a/2$ plane (or in the two $z=-a/4$ and $z=5a/4$ planes): In these cases, the Hartree energy would in fact reduce to the electrostatic energy of two (or three) charged planes.